Lehrer, S. S. (1971) *Biochemistry 10*, 3254–3262.
Longworth, J. W. (1971) in *Excited States of Proteins and Nucleic Acids* (Steiner, R. F., & Weinryb, I., Eds.) pp 319–485, Plenum Press, New York and London.
McClure, O. W., & Edelman, G. M. (1967) *Biochemistry 6*, 559–566.
Palmer, T. E., & Neet, K. E. (1980a) *J. Biol. Chem. 255*, 5170–5176.
Palmer, T. E., & Neet, K. E. (1980b) *Arch. Biochem. Biophys. 205*, 412–421.
Parker, C. A. (1968) *Photoluminescence of Solutions*, pp 220–222, Elsevier, New York.
Pattison, S. E., & Dunn, M. F. (1975) *Biochemistry 14*, 2733–2739.
Ramachandran, L. K. (1962) *J. Sci. Ind. Res. 21C*, 111.
Ramachandran, L. K., & Witkop, B. (1959) *J. Am. Chem. Soc. 81*, 4028.
Schachman, H. K. (1959) in *Ultracentrifugation in Biochemistry*, p 82, Academic Press, New York.
Schmir, G. L., & Cohen, L. A. (1961) *J. Am. Chem. Soc. 83*, 723.
Shinidzky, M., & Goldman, R. (1967) *Eur. J. Biochem. 3*, 139–144.
Smith, A. (1969) Ph.D. Dissertation, Stanford University, University Microfilms, Ann Arbor, MI.
Smith, A. P., Varon, S., & Shooter, E. M. (1968) *Biochemistry 7*, 3259–3268.
Spande, T. F., & Witkop, B. (1967) *Methods Enzymol. 11*, 498–506.
Spande, T. F., Green, N. M., & Witkop, B. (1966) *Biochemistry 5*, 1926–1933.
Stach, R. W., Server, A. C., Pignatti, P. F., Piltch, A., & Shooter, E. M. (1976) *Biochemistry 15*, 1455–1461.
Teale, F. W. J. (1960) *Biochem. J. 76*, 381–388.
Thomas, A. K., Baglan, N. C., & Bradshaw, R. A. (1981a) *J. Biol. Chem. 256*, 9156–9166.
Thomas, A. K., Silverman, R. E., Jeng, I., Baglan, N. C., & Bradshaw, R. A. (1981b) *J. Biol. Chem. 256*, 9147–9155.
Varon, S., Nomura, J., & Shooter, E. M. (1967) *Biochemistry 6*, 2202–2209.
Varon, S., Nomura, J., & Shooter, E. M. (1968) *Biochemistry 7*, 1296–1303.

Nuclear Magnetic Resonance Studies of Xenon-129 with Myoglobin and Hemoglobin†

R. F. Tilton, Jr., and I. D. Kuntz, Jr.*

ABSTRACT: Nuclear magnetic resonance studies of ^{129}Xe are consistent with one kinetically distinguishable binding environment in methemoglobin and two in metmyoglobin. The Xe binding site in methemoglobin is assigned to a cavity formed by the A–B and G–H corners of the globin chain [Schoenborn, B. P. (1965) *Nature (London) 208*, 760–762]. The small differences between α-hemoglobin and β-hemoglobin are not resolved by the NMR experiments. The Xe association rate constant at 18 °C with methemoglobin is greater than 6×10^7 M^{-1} s^{-1} with an activation barrier of approximately 13 kcal/mol. One of the binding sites in metmyoglobin is associated with a cavity on the proximal side of the porphyrin ring, opposite the O_2 binding site [Schoenborn, B. P., Watson, H. C., & Kendrew, J. C. (1965) *Nature (London) 207*, 28–30]. An estimate of the association rate constant of Xe at 18 °C is 1×10^7 M^{-1} s^{-1} with an activation barrier of approximately 16 kcal/mol. The second metmyoglobin binding site has similar NMR and kinetic properties of those for methemoglobin.

Myoglobin and hemoglobin bind xenon in specific relatively nonpolar cavities within the protein matrix. X-ray crystallographic studies reveal that sperm whale metmyoglobin binds xenon in the proximal cavity equidistant between the coordinated proximal histidine (F8) and a pyrrole group of the heme ring (Schoenborn et al., 1965). A second binding site has been reported in sperm whale alkaline myoglobin (pH 9.4) (Schoenborn, 1969). The location of this cavity is similar to the binding site found in horse hemoglobin—a cavity formed by the G–H and A–B helix corners close to the external surface (Schoenborn, 1965) (Figure 1). Equilibrium binding studies are consistent with a single association constant for Xe–hemoglobin complex on the order of 200 M^{-1} (Conn, 1961). The Xe–metmyoglobin interaction is better described with two association constants of approximately 190 M^{-1} and 10 M^{-1} (Ewing & Maestas, 1970). While these studies contain structural and thermodynamic information, they reveal little about the dynamics of Xe binding. Inspection of the protein crystal structures makes it clear that the Xe binding sites are inaccessible to ligand without cooperative protein motions to allow transient passage. The dynamics of Xe binding can be used to probe these protein motions. Kinetic studies have been made of the protein barriers associated with the binding of O_2 and CO to deoxymyoglobin by using optical techniques (Austin et al., 1975); however, Xe is an inert ligand that offers some unique features for probing barriers associated with a different class of binding sites, and its motion can be monitored directly by Xe NMR.

The use of NMR in studying chemical exchange is well established (Emsley et al., 1965). Kinetic information is contained in the transverse relaxation times and hence in the line shape of the resonance peak. Depending on the exchange rates and the chemical shifts, a process can be described as being in slow, intermediate, or fast exchange. In the limit of slow exchange a separate resonance is observed for each environment. For two sites this condition is met when $(\tau\Delta\omega)^2 \gg 1$ where τ is the lifetime of state and $\Delta\omega = 2\pi\Delta\nu$ with $\Delta\nu$

† From the Department of Pharmaceutical Chemistry, University of California, San Francisco, California 94143. *Received June 9, 1982.* This work was supported by the National Institutes of Health and the Academic Senate, University of California.

0006-2960/82/0421-6850$01.25/0

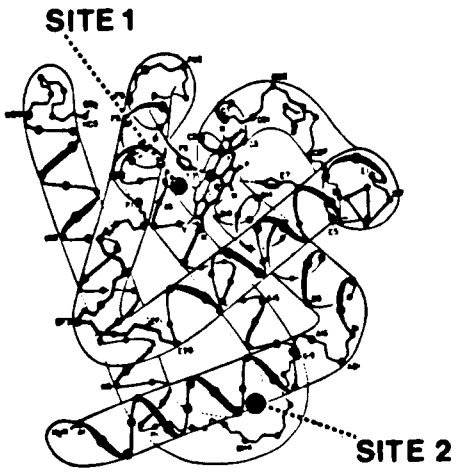

FIGURE 1: Approximate location of the Xe binding sites within the globin matrix. Crystalline metmyoglobin binds Xe at site I, alkaline myoglobin at sites I and II, and methemoglobin at site II (after Schoenborn).

the chemical shift difference between the two states. The line width of each resonance is given by

$$\pi\Delta\nu_i = \frac{1}{T_{2i}} + \frac{1}{\tau_i}$$

where T_2 is the intrinsic transverse relaxation time for each environment. As the exchange rate increases, the line width increases, reaching a maximum when the resonances finally coalesce into a single broad peak at intermediate exchange $(\tau\Delta\omega)^2 \sim 1$. The population average resonance sharpens as τ decreases further until the fast-exchange condition $(\tau\Delta\omega)^2 \ll 1$ is reached. In fast exchange the line width is given by

$$\pi\Delta\nu = \frac{1}{T_2} = \frac{P_A}{T_{2A}} + \frac{P_B}{T_{2B}} + P_A^2P_B^2(\Delta\omega)^2(\tau_A + \tau_B)$$

where P_A, P_B, T_{2A}, T_{2B}, τ_A, and τ_B are the populations, intrinsic transverse relaxation times, and lifetime of states A and B, respectively. Two contributions are observed: a component due to the natural line width in each environment (the line width in the absence of chemical exchange) and a component due to the partial residency during chemical exchange. A treatment of the two-site, fast-exchange mechanism for complex formation protein + Xe $\rightleftarrows$ protein$\sim$Xe shows that the line width due to exchange can be described by

$$\Delta W \approx \frac{P_A(1 - P_A)^2 4\pi(\Delta\nu_{AB})^2}{k_{off}} \quad (1)$$

where P_A is the fraction of ligand bound by protein, $\Delta\nu_{AB}$ is the limiting chemical shift difference in hertz between the bound and free ligand, K_{off} is the dissociation rate of the complex, and ΔW is the exchange-dependent line-width contribution. The frequency shift at maximum line width is one-third of $\Delta\nu_{AB}$. Hence, in principle, a determination of the conditions for maximum line broadening is sufficient to determine ΔW and $\Delta\nu_{AB}$ and thereby to calculate k_{off}. Equation 1 has been shown to be accurate to 5% in cases where $\Delta W \leq \Delta\nu_{AB}/3$ (Sudmeier et al., 1980). An initial study of Xe in biological materials by Miller et al. (1981) showed that Xe was in fast exchange in cyanometmyoglobin solutions.

Experimental Procedures

Materials. Sperm whale myoglobin (type II salt-free lyophilized powder) and human hemoglobin (type IV 2× crystallized and lyophilized) were purchased from Sigma and used without further purification. Xenon gas (Research Grade) was purchased from Airco. Deuterated solvents were from Aldrich. High-pressure NMR tubes were custom-made by Wilmad with o.d. 12 mm and i.d. 9 mm and were provided with a high-pressure stopcock and vacuum line connections. For the experiments at atmospheric pressure, we used standard thin-wall 12-mm tubes from Wilmad.

Instrumentation. Nuclear magnetic resonance spectra were obtained on a Varian XL-100 by using a 12-mm Multi Observational Nuclear Accessory (MONA) probe (Nicolet) tuned to the ^{129}Xe resonance frequency of 27.682 MHz. Standard parameters used were spectral width ±2000 Hz, delay time 180 μs, 2K spectral points, and a recycle time of 0.256 s. The 90° pulse was 36 μs for the thick wall NMR tubes. Block averaging of NMR scans was done when more than 30 000 acquisitions were needed. Line widths were determined by a computer program that fits the NMR signal to a single Lorentzian band shape. Temperature control was maintained throughout all experiments, varying ±0.2 °C during data acquisition and maintained at 18 ± 0.5 °C for all of the fast-exchange experiments. Temperature control at subzero temperatures was within ±2 °C. Probe temperatures were measured with a Fluke 2100A digital thermometer. Protein concentrations were determined on a CARY 118 UV–vis spectrometer.

Procedure. Protein solutions were freshly prepared by dissolving lyophilized protein in 30% D_2O and 70% doubly distilled H_2O with self-buffering at pH 6.9. Nominal protein concentrations ranged between 1% and 40% by weight. Samples were centrifuged and filtered through glass wool to remove particulates. Final protein concentrations were determined by appropriate dilution (OD < 1) with absorbence monitored at 280 nm ($\epsilon_{280} = 3.1 \times 10^4$; Breslow, 1964). The deoxy, ferric cyano, and carbon monoxy derivatives of myoglobin and hemoglobin were produced by standard methods described in the literature (Smith & Williams, 1968; Samejima & Yang, 1964).

Xenon was added by flushing 1 volume of gas through the tube followed by gentle agitation and then a final flushing of 2–3 more volumes of gas to produce the 1-atm samples. Higher pressure samples (2–10 atm) were made on a vacuum line by condensing an appropriate known gas volume into the smaller volume of the NMR tube cooled in liquid N_2. The solid Xe–protein sample was then warmed to room temperature and gently swirled to ensure equilibration. The equilibration time was generally 30 min, and the samples were not spun. The 90° NMR pulse was determined with a sample containing 70% C_6H_6–30% C_6D_6 equilibrated with 1 atm of Xe. One pulse gave a S/N of 4 for this sample and a T_1 of 200 s.

Low-temperature studies used a cold N_2 gas cooling system. Dry protein was dissolved at −10 °C in a solvent of 20% H_2O, 30% D_2O, 25% MeOH, and 25% ethylene glycol (freezing point −50 °C) with 2×10^{-4} M $MnCl_2$ added as a paramagnetic relaxation agent. These samples were stored at −20 °C when not in the probe. Titrations with HgI_3^- were done by rapid dilution of 1.0 M $KHgI_3$ into the protein solution.

Results

We present our results in four sections. In the first section we describe the effects on the Xe resonance of the Fe oxidation and spin state in both hemoglobin and myoglobin. In the second section we present low-temperature studies (0 to −45 °C) that demonstrate fast, intermediate, and slow exchange of Xe with myoglobin and hemoglobin. In the third section we report the effects of HgI_3^- on the Xe resonance in myoglobin. In the last section we make a semiquantitative assessment of kinetic parameters by measuring the chemical shift

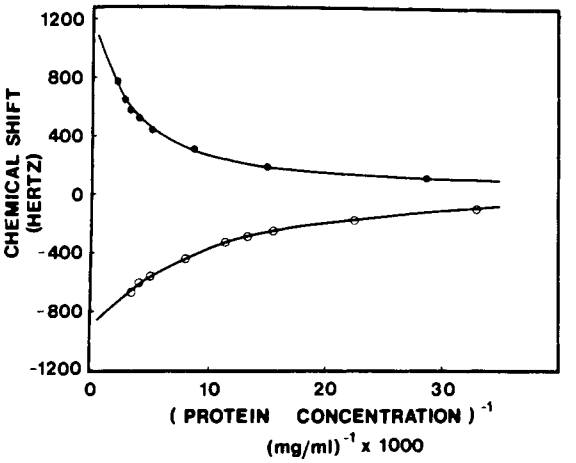

FIGURE 2: ^{129}Xe chemical shift vs. reciprocal protein concentration for metmyoglobin (●) and methemoglobin (○) solutions. The chemical shift is referenced to the xenon resonance in water.

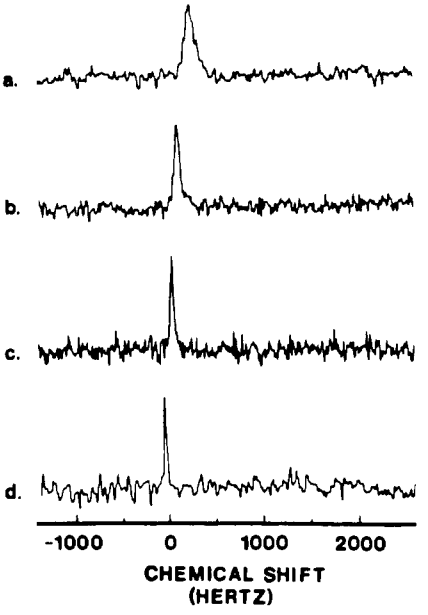

FIGURE 3: ^{129}Xe spectra at 18 °C: (a) metmyoglobin; (b) deoxymyoglobin; (c) ferric cyanometmyoglobin; (d) (carbon monoxy)myoglobin. Spectrometer settings as given in text. Protein concentration 100 mg/mL, Xe pressure 1 atm.

and line width dependence of the Xe resonance as a function of both protein and Xe concentrations in the fast-exchange regime.

(I) Overview. For temperatures above 0 °C, at Xe pressures of 1–10 atm, and at protein concentrations of 10–300 mg/mL, we observe a single Lorentzian-shaped Xe resonance with chemical shifts that vary smoothly with the concentration of either myoglobin or hemoglobin (Figure 2). Extrapolation of these curves to infinite protein concentration give a limiting chemical shift of 1200 Hz upfield for Xe in metmyoglobin and 900 Hz downfield for Xe in methemoglobin relative to the chemical shift of Xe in water. These observations are consistent with Xe being in fast exchange on the NMR time scale between at least two distinctive environments which we will call protein and solvent. We further observe (Figure 3) that both the chemical shifts and line widths of Xe are sensitive to changes of the Fe oxidation and spin state in both proteins. In particular, the Xe resonance in myoglobin is shifted the most upfield from the water reference in the met state (Fe^{3+}, $S = {}^5/_2$), to lower field in deoxymyoglobin (Fe^{2+}, $S = 2$), and is shifted downfield relative to water in both ferric cyanomyoglobin (Fe^{3+}, $S = 1/2$) and (carbon monoxy)myoglobin (Fe^{2+}, $S = 0$). Along with this progressive downfield shift upon reduction of the paramagnetic Fe to the diamagnetic state is a considerable narrowing of the line width. The Xe chemical shift in the presence of hemoglobin, on the other hand, is shifted downfield from water for all samples and is relatively insensitive to changes in the Fe spin state or oxidation state. Similarly the line width undergoes only a slight broadening upon reduction from met- to deoxyhemoglobin and then a slight narrowing upon cyano or CO ligation. These results are summarized in Table I.

Table I: Sensitivity of ^{129}Xe Resonance to Fe Oxidation and Spin State[a]

sample	Fe state	$\Delta\nu$ (Hz)[b]	ΔW (Hz)
metmyoglobin	Fe^{3+}, $S = {}^5/_2$	192	90
deoxymyoglobin	Fe^{2+}, $S = 2$	49	45
ferric cyanomyoglibin	Fe^{3+}, $S = {}^1/_2$	−20	17
(carbon monoxy)myoglobin	Fe^{2+}, $S = 0$	−45	20
methemoglobin	Fe^{3+}, $S = {}^5/_2$	−292	10
deoxyhemoglobin	Fe^{2+}, $S = 2$	−288	21
ferric cyanohemoglobin	Fe^{3+}, $S = {}^1/_2$	−305	10
(carbon monoxy)hemoglobin	Fe^{2+}, $S = 0$	−286	15
water		0	4

[a] Protein concentration 100 mg/mL, xenon pressure of 1 atm, 18 °C. [b] $\Delta\nu$ is the chemical shift difference between Xe in the protein and Xe in water. ΔW is the width at half-height of the resonance peak.

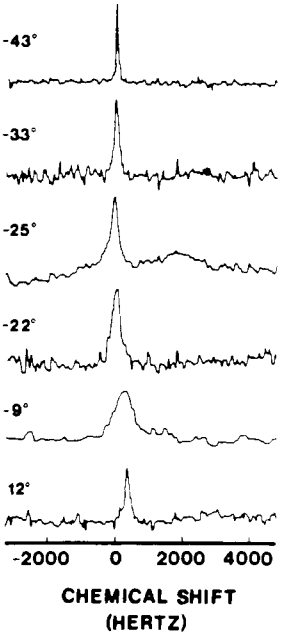

FIGURE 4: ^{129}Xe spectra at variable temperatures. Metmyoglobin concentration 130 mg/mL, Xe pressure 1 atm (at 18 °C).

(II) Low Temperature. Low temperature was used to slow the exchange between solvent and protein sites. Studies were done in the cryoprotecting solvent. Low-temperature UV–vis spectra of the protein samples indicate only minor differences from the room temperature aqueous spectra. Representative NMR spectra of Xe in metmyoglobin solutions as a function of temperature are shown in Figure 4. Qualitatively, we observe that the Xe resonance broadens and shifts downfield as the temperature is lowered from +12 to −9 °C. The line then begins to narrow with constant chemical shift until −25 °C where we observe two peaks: a downfield sharp resonance and a broad band 1800–2000 Hz upfield. When the tem-

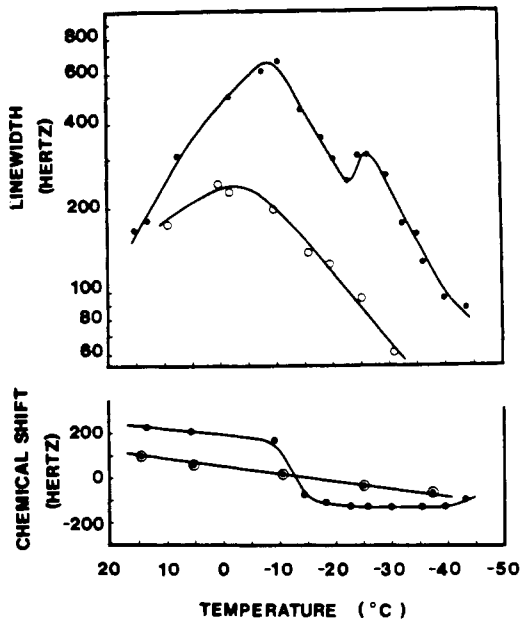

FIGURE 5: (Upper panel) Temperature dependence of ^{129}Xe line width for metmyoglobin solution [130 mg/mL (●)] and HgI_3^--treated (○) sample. (Lower panel) Temperature dependence of ^{129}Xe chemical shift in cryosolvent (⊙) and metmyoglobin solution (●).

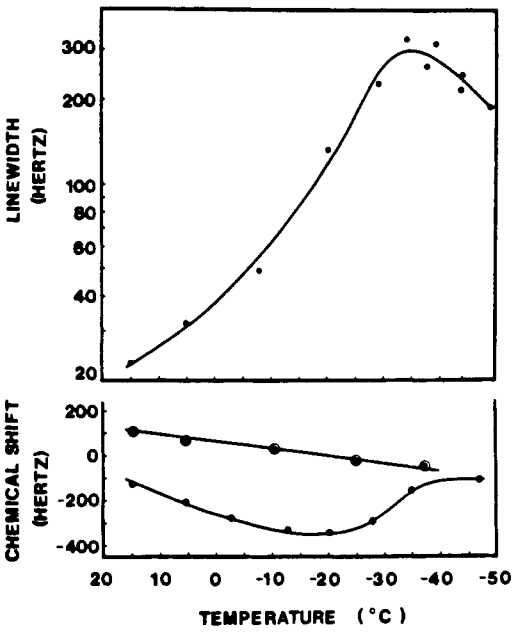

FIGURE 6: (Upper panel) Temperature dependence of ^{129}Xe line width in methemoglobin solution (●). (Lower panel) Temperature dependence of ^{129}Xe chemical shift in cryosolvent (⊙) and methemoglobin solution (●).

perature is lowered further, the downfield resonance continues to narrow and the upfield band disappears. The disappearance of the broad component probably rests on achieving complete slow exchange and on the strong temperature dependence of the solution viscosity at these low temperatures. A plot of line width and chemical shift of the sharper Xe resonance as a function of temperature is given in Figure 5. There are two line broadening events: one which reaches a maximum of 700 Hz at −10 °C and the other of 300 Hz at −25 °C. Correspondingly there is a large downfield chemical shift at −12 °C and a small upfield shift at −45 °C. The experiment was terminated at −50 °C due to freezing of the cryosolvent. A similar experiment using methemoglobin indicates only a single broad maximum in the line width at −35 °C with a large upfield shift toward pure solvent between −27 and −50 °C (Figure 6). We tentatively conclude that two distinct binding sites are required to explain the myoglobin results. We associate the major broadening event at −10 °C with site I and the secondary broadening event at −25 °C with site II. The hemoglobin results can be explained with a single binding site.

(III) Competitive Binding of HgI_3^- and Xe in Metmyoglobin. X-ray crystallographic studies have indicated that HgI_3^- and Xe can occupy the proximal binding cavity of metmyoglobin (Kretsinger et al., 1968). Competitive binding with Xe was observed when we titrated solutions of metmyoglobin with HgI_3^- (Figure 7). Increasing amounts of HgI_3^- move the Xe resonance downfield, reaching a limiting chemical shift at a 1:1 stoichiometry of Hg to protein. In all cases we observe that the limiting chemical shift is downfield from that of the aqueous reference solution and that the limiting chemical shift is proportional to the protein concentration. The line width of the Xe resonance at stoichiometric HgI_3^- binding is also substantially narrowed to 20–30 Hz. Our low-temperature studies of 2:1 Hg:protein in cryosolvent reveal a single line-broadening event with a maximum line width of 250 Hz occurring at −6 °C (Figure 5). From these results we believe that the site being blocked by HgI_3^- is site I.

(IV) Fast Exchange. To determine the Xe exchange rate, we have measured the chemical shifts and line widths of the xenon resonance as a function of both protein and Xe concentrations at 18 °C. Our most extensive studies used metmyoglobin. The Xe chemical shift moves downfield (toward solvent) at higher Xe gas pressures, consistent with lower fractional binding. The variation of line width with Xe pressure is more complex (Figure 8). At low protein concentrations the Xe resonance sharpens with increasing Xe pressures while at high protein concentrations the line broadens with increasing pressure. These effects are in qualitative accord with the simple two-site exchange theory, but a quantitative treatment requires that we isolate the exchange-related line broadening from other sources such as bulk viscosity and magnetic field inhomogeneities. To estimate these corrections we have compared the Xe line widths in solutions of different protein concentrations that have similar chemical shifts. We then calculate the line-width corrections needed to bring the results at each protein concentration into correspondence. These corrections are approximately linear in protein concentration and when applied to the raw data of Figure 8 produce the data along the smooth curve. If we now fit the corrected data to the functional form of eq 1, we find ΔW, the exchange-related broadening, to be 75 Hz and $\Delta\nu_{AB}$,

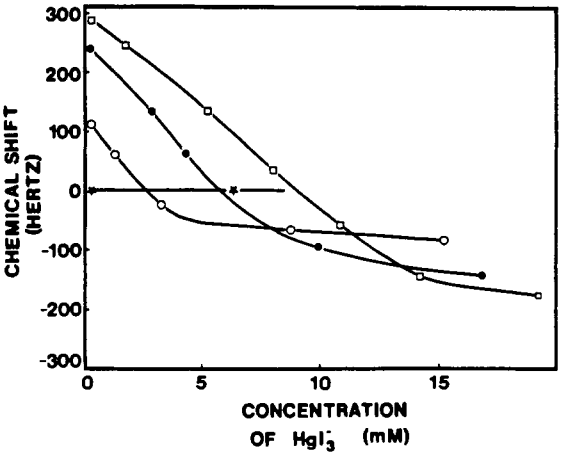

FIGURE 7: Titration of ^{129}Xe chemical shift in metmyoglobin solutions of (○) 35, (●) 90, and (□) 130 mg/mL with $KHgI_3$, 18 °C, at 1 atm of Xe pressure. Solvent chemical shift (★).

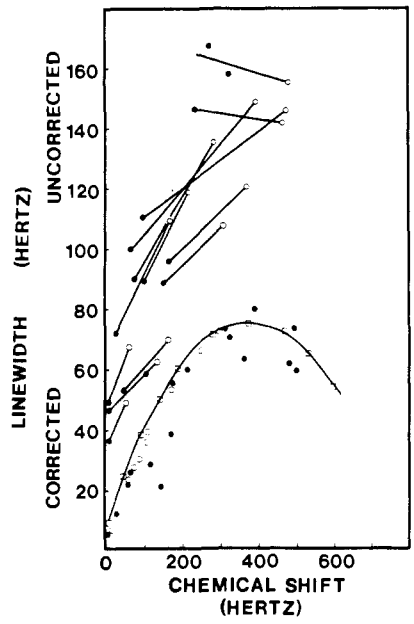

FIGURE 8: (Upper portion) Uncorrected line widths of ^{129}Xe at various pressures and metmyoglobin concentrations plotted against chemical shift of ^{129}Xe. Lines indicate constant protein concentrations. Xe pressure: (○) 1 atm; (●) greater than 1 atm. (Lower portion) Line widths corrected for viscosity effects as described in text. Open circles are data used to establish the correction. The line-width dependence of eq 1 is given by the solid line and the squares; the theoretical curve is scaled to the maximal corrected line width.

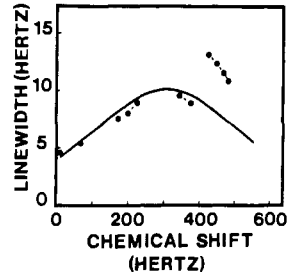

FIGURE 9: Measured line widths of ^{129}Xe in methemoglobin solutions at various protein concentrations and Xe gas pressures. The solid line is only a guide for the eye.

the limiting chemical shift, to be 3 × (380) or 1140 Hz. The limiting chemical shift measured in this way is in good agreement with the chemical shift extrapolated from the protein concentration dependence of 1200 Hz (Figure 2).

A similar study has been done for methemoglobin. The general features of the Xe line width dependence on Xe gas pressure and protein concentration are similar to those in metmyoglobin, but the line widths are much sharper being less then 15 Hz (Figure 9). Due to this small exchange dependence, we cannot use the same data reduction method. Instead we simply place an upper bound of 5 Hz for ΔW, the exchange contribution to the Xe line width, in methemoglobin solutions. The limiting chemical shift, taken as 3 times the chemical shift at the maximum line width is ~1000 Hz in fair agreement with the extrapolated chemical shift of 870 Hz (Figure 3).

(V) Calculations of Equilibrium Constants, Rate Constants, and Associated Barriers. From our data we can estimate an equilibrium constant (K_a) by assuming a simplified two-site exchange, protein + Xe ⇄ protein~Xe. K_a can then be expressed as

$$\frac{P_A}{P_T - P_A P_T - P_A[Xe]}$$

where P_A is the fraction of Xe bound, P_T is the total protein concentration, and [Xe] is the "free" Xe concentration in solution. The maximum of the line-broadening curve is found at a protein concentration of 150 mg/mL (0.009 M) and at a Xe concentration of 0.005 M. Theoretically, the maximum occurs at a fraction bound of $^1/_3$, yielding a K_a of 77 M^{-1}. This value is considerably less than the equilibrium binding results in the literature of 200 M^{-1} and may reflect the averaging of both a high- and low-affinity binding site (Ewing & Maestas, 1970).

Table II: Dependence of k_{off} (s^{-1}) on $\Delta\nu_{AB}$ and ΔW

metmyoglobin				methemoglobin		
ΔW	$\Delta\nu_{AB}$ (Hz)			ΔW	$\Delta\nu_{AB}$ (Hz)	
(Hz)	1200	1900	2000	(Hz)	900	1000
75	3.6×10^4	8.9×10^4	9.9×10^4	8	1.9×10^5	2.3×10^5
67	4.0×10^4	1.0×10^5	1.1×10^5	5	3.0×10^5	3.7×10^5
60	4.5×10^4	1.1×10^5	1.2×10^5	3	5.0×10^5	6.2×10^5

From our fast-exchange data and eq 1 we can estimate the dissociation rate constants of Xe from both hemoglobin and myoglobin. For hemoglobin with only a single apparent binding site, the procedure is straightforward. Solving eq 1 for k_{off} and using $P_a = {}^1/_3$, an upper limit for ΔW of 5 Hz, and $\Delta\nu_{AB}$ of 900 Hz, we find a lower limit for k_{off} of 3.0×10^5 s^{-1}. This result and the published value for K_a of 200 M^{-1} yield a lower limit for the on-rate constant of Xe with methemoglobin of 6.0×10^7 M^{-1} s^{-1}. The rate constant calculations for metmyoglobin are complicated by the likelihood of multiple binding sites. We assume from the HgI_3^- competition studies that the limiting chemical shifts of 1150 and 1200 Hz for Xe associated with site I at room temperature are underestimates. A larger limiting chemical shift of 1900 Hz is indicated by the low-temperature slow-exchange spectrum. Similarly, we expect that the observed ΔW will have contributions from chemical exchange from both sites. Therefore, to make our estimations of the rate constants for Xe binding at site I, we use for $\Delta\nu_{AB}$ the slow-exchange limit of 1900 Hz and a ΔW of 70 Hz, the observed value with a 5-Hz correction based on the similarity of features with hemoglobin (see Discussion). These values in eq 1 yield a k_{off} of 9.6×10^4 s^{-1}. With a published K_a of 190 M^{-1}, we then calculate the association rate constant to be 1.8×10^7 M^{-1} s^{-1}. While we feel that these are reasonable approximations, we illustrate in Table II the sensitivity of the dissociation rate constants to other choices for ΔW and $\Delta\nu_{AB}$.

Finally we are able to make a crude estimate of the barriers associated with Xe binding. From intermediate-exchange theory we can approximate the residence time τ at the coalescence point to be equal to $\tau = 2(2^{1/2}/\Delta\omega)$. For metmyoglobin we calculate τ to be 2.3×10^{-4} s at −10 °C and for methemoglobin to be 4×10^{-4} s at −35 °C. When the fast-exchange values for k_{off} as calculated above are used, these τ's at 18 °C are 1×10^{-5} and 3×10^{-6} s for metmyoglobin and methemoglobin, respectively. Assuming the Arrhenius equation applies and that both the preexponential factor and the activation barrier E_A are temperature independent, one can calculate using only these two points, activation energies of 16 and 13 kcal/mol, respectively, with an uncertainty of a few kcal/mol. While these barriers are approximations, they are consistent with the faster exchange rates observed for the hemoglobin–Xe complex compared with the myoglobin–Xe system.

Discussion

We first deal with the problem of assigning the binding sites detected by NMR with those reported in the crystallographic

studies in both myoglobin and hemoglobin. It seems clear that the myoglobin results (Figures 5 and 7) require at least two distinct binding sites, while the hemoglobin results do not. The direct dependence of the Xe chemical shift in the myoglobin solutions on the Fe spin state place one of the Xe binding sites near the iron atom. This is corroborated by the finding that the proton resonance of a porphyrin methyl group is shifted upon binding of Xe (Shulman et al., 1970). The simplest interpretation is that the binding site is the same one found in the metmyoglobin X-ray crystallographic studies, i.e., equidistant between the proximal His (F8) and the porphyrin ring on the opposite side from the O_2 binding site (site I). This interpretation is strengthened by the observation that HgI_3^-, which is known to bind in this site, competes with the iron-sensitive Xe resonance. Partial Xe occupancy of the distal cavity would also yield an iron-sensitive resonance, but there is no direct evidence for this idea. The second site in myoglobin is characterized by a narrow line, a downfield shift similar to that found in methemoglobin, and an NMR signal which is little affected by changes in Fe oxidation or spin state. While the evidence is circumstantial, we suggest that the second binding site is the one observed in X-ray crystallographic studies of methemoglobin and alkaline myoglobin—a cavity formed roughly by the G–H and A–B helix corners (site II). A more direct approach is to compete for this site with $AuCl_4^-$ which is known to bind in this cavity from X-ray crystallographic studies (Bluhm et al., 1958). Our initial attempts with $AuCl_4^-$, however, caused precipitation of the protein.

Our low-temperature studies of metmyoglobin indicate two line-broadening events. We associate one event with each Xe binding site. On the basis of maximal line broadening of 250 Hz observed in low-temperature studies of the Xe line width in the HgI_3^-–metmyoglobin complex, we assign the broadening event at −25 °C to site II. The similarity with the low-temperature line-width results for methemoglobin supports this assignment. The larger broadening event at −9 °C is then associated with exchange at site I. These assignments are also consistent with the downfield chemical shift at −10 °C and the upfield chemical shift at −45 °C. The difference in the coalescence point for site II in metmyoglobin (−25 °C) and HgI_3^-–metmyoglobin (−6 °C) suggests that the HgI_3^- alters the exchange kinetics by, for example, tightening the metmyoglobin structure.

An alternate explanation for the two line-broadening events of the metmyoglobin sample is that the low-temperature conditions cause a cooperative transition in the protein conformation, altering protein barriers and hence exchange rates. No such transition is observed in our UV–vis spectra nor has one been reported. Given these site assignments, we attribute the upfield chemical shift of Xe bound at site I primarily to paramagnetic effects of the iron and the downfield shift of Xe bound at site II to deshielding effects of charged or aromatic residues, particularly His-24, His-119, and Trp-14.

Our conclusion that there are two sites for Xe in metmyoglobin while only one site was seen with X-ray crystallography bears some examination. There are two likely possibilities. The first is that site II exists but has low occupancy which cannot be detected crystallographically in metmyoglobin crystals at room temperature but which, under the proper conditions, can be detected by solution NMR. The second possibility is that the crystallizing conditions of high salt disrupt binding at site II by direct electrostatic interaction or by perturbing the crystal structure, especially in the flexible G–H helix corner.

The Xe–methemoglobin low-temperature data show a single line-broadening event and a broad temperature range (−20 to −40 °C) for the chemical shift transition. This observation is consistent with a class of binding sites that are not resolved on a kinetic basis. X-ray crystallography suggests a small inequivalence between the α- and β-chain Xe binding sites, although both sites are in the region of the A–B and G–H corners. As with site II in metmyoglobin, they show a downfield chemical shift and a narrow Xe resonance line width. The downfield shift may arise from the deshielding effects of the amino acid residues Lys-11, Trp-14, Phe-117, and His-112 in the α chain and Lys-8, Trp-15, Phe-118, His-116, and His-117 in the β chain.

The quantitative accuracy of the kinetic results rests on three assumptions: the initial use of a two-site exchange model to interpret the data, the approximations of eq 1 in calculating the rate constants, and the validity of our data reduction method. The two-site model appears to be a reasonable first approximation for the Xe–hemoglobin complex. However, in metmyoglobin, the evidence is strong for at least three sites. Rather than attempting a full three-site analysis of the NMR data, we have made some simple first-order corrections to separate the large site I effects from the much smaller site II terms. These corrections are based on the similarity of the binding environments and exchange kinetics (i.e., the chemical shift and the line widths) of metmyoglobin site II and the methemoglobin binding site. Furthermore the myoglobin binding site II is believed to be the lower affinity (10 M^{-1}) binding site based on lower occupancy, observed in X-ray crystallographic studies of alkaline myoglobin. Hence it would contribute a proportionately smaller amount to the exchange-induced line width. A reasonable guess for the exchange contribution of site II is approximately 5–10% of the observed line-width change, and we have used a correction of 5 Hz at 18 °C.

The second assumption is the validity of eq 1 in calculating the kinetic off rate. In the derivation of this equation the intrinsic transverse relaxation times of Xe in solvent and bound to protein were taken to be either long or of comparable magnitude so that concentration-dependent line broadening will be due only to chemical exchange and not relative occupancy. However, if one intrinsic T_2 is much shorter than the other, it will also make a concentration-dependent contribution to the line width. In principle these two terms can be separated since a site-specific T_2 will contribute in direct proportion to occupancy (P_A) while the exchange terms will contribute as $P_A(1 - P_A)^2$. As indicated by the maximum in the line width vs. P_A plot, there must be a strong exchange contribution (Figure 8). Furthermore a large linear contribution would shift the exchange-related maximum from the true $P_A = {}^1/_3$, resulting in a limiting chemical shift that would be greater then the extrapolated value from the concentration studies (Figure 2). This is not observed. While this reasoning suggests a relatively small contribution to the line width from the intrinsic T_2's, it would be more satisfactory to measure T_1 and T_2 directly.[1]

The inherent assumption in our data correction procedure is that the chemical shift is only sensitive to the fractional population of Xe in each site and is insensitive to field inhomogeneities and viscosity terms that affect the line width. Further, we assume that the limiting chemical shift of the

[1] A preliminary measurement of T_1 for Xe–metmyoglobin solutions of 10–15 ms suggests corrections of about 10 Hz, which would increase the metmyoglobin rate constants by roughly 15%. Sites with T_1's greater than 1 s would not have been detected by our procedures.

Table III: Kinetic Parameters for Xe, CO, and O_2 with Myoglobin and Hemoglobin

	k_{on} (M^{-1} s^{-1})	k_{off} (s^{-1})	activation enthalpy (kcal/mol)
myoglobin			
Xe (site 1)	1.9×10^7 [a]	1.0×10^5 [a]	~17 [b]
CO	5.0×10^5 [c]	1.5×10^{-2} [c]	11-24 [d]
O_2	1.5×10^7 [c]	10 [c]	12-16 [d]
hemoglobin			
Xe	6.0×10^7 [a]	3.0×10^5 [a]	~13 [b]
CO	4.6×10^6 [c]	~1-10 $\times 10^{-2}$ [c]	
O_2	3.3×10^7 [c]	15 [c]	

[a] For uncertainty estimates see Table II and text. [b] For uncertainty estimates see text. [c] Parkhurst (1979). [d] Austin et al. (1975).

"bound" state is independent of protein or Xe concentration. The effect of field inhomogeneities on chemical shift can be eliminated since spinning and nonspinning samples have essentially identical chemical shifts and line widths. A more crucial assumption is that chemical shift changes with Xe pressures and protein concentrations are due to population changes at one binding site or a kinetically equivalent set of binding sites, i.e., that there is a direct proportionality between chemical shift and occupancy. In fact we have argued from our low-temperature data that a second protein site can be detected, but the line-width and chemical shift contributions from this second site are smaller under fast-exchange conditions.

Accepting the assumption that the chemical shift of Xe is a monitor of the fraction of Xe bound to a specific site, we can ascribe the line-width difference between two samples with the same chemical shift to nonexchange related line-broadening effects. Finally, if these line-broadening contributions are not dependent on Xe pressure, this same correction can be applied to all data points of the same protein concentration. The reasonable fit between the theoretical curve and our corrected curve (Figure 8) substantiates the validity of these assumptions.

With these reservations we were able to estimate the Xe association rates for hemoglobin and myoglobin and found that they are on the same order (10^6–10^7 M/s) as those for gaseous ligands which bind to the distal binding cavity (Antonini & Brunori, 1971). In particular we find that the Xe association rate is at least 3 times faster with hemoglobin then with myoglobin site I. The Xe association rates are 1–2 times faster in both hemoglobin and myoglobin than those for O_2 but are 10 times faster in hemoglobin than those for CO and 40 times faster in myoglobin (Table III). We stress that our association rates for hemoglobin are lower limits, and all our association rates are with the met protein rather than the deoxy proteins.

While our NMR techniques are not able to distinguish multiple or sequential barriers we are still able to make a crude calculation of a rate-limiting barrier for binding to each site. A comparison with the barriers to CO and O_2 binding calculated from low-temperature flash photolysis studies indicates fair agreement with the barriers calculated for Xe binding (Table III). Whether these association rates and barriers are "typical" values for specific gaseous ligand binding is still uncertain, but clearly different binding cavities within the protein matrix can have similar binding kinetics. On the other hand, our results do not seem consistent with the fluorescent quenching studies that indicate O_2 association rates and barriers much closer to the diffusion controlled limit of 10^9–10^{10} M^{-1} s^{-1} and 3.5 kcal/mol (Lakowicz & Weber, 1973). At this time we can only point out that the two processes are measuring different phenomena, i.e., binding to a specific protein site and nonspecific quenching of an optical excited state of tryptophan within the protein matrix, and hence may not be comparable.

An important question which has not been addressed in this paper is the possible binding pathways which Xe may traverse in reaching the binding cavity. While our NMR techniques do not hold much promise of elucidating a pathway, there is some evidence from variable low-temperature crystallographic studies of myoglobin that the vibrational and conformational fluctuations of the proximal side of the heme (residues 42, 43, 89, 92, 97, 99, 103, 104, and 138) allow greater motion than that observed on the distal side (residues 39, 64, 67, 68, 71, and 107) (Frauenfelder et al., 1979). If ligand binding is indeed controlled by concerted protein gate dynamics, one might then predict that while only a few pathways exist for CO and O_2 passage, Xe may be able to follow a variety of energetically similar pathways via routes between the F, G, and H helices. We have some indication that there is a larger proliferation of small channels (less than 1.00-Å radius) on the proximal side than on the distal side, and future studies will be directed at answering this question more directly (I. D. Kuntz, and N. Max, and R. F. Tilton, unpublished results).

Conclusion

^{129}Xe is a sensitive NMR probe for heme proteins. The large chemical shift range and good sensitivity can be exploited to reveal information about specific binding sites as well as Xe binding dynamics. Since the Xe binding sites are in different locations within the protein matrix, this information is complimentary to gaseous ligand binding with the O_2 site but without the added complications of specific binding site chemistry. Our NMR results indicate the following:

(1) Metmyoglobin in solution has two Xe binding environments. One of these environments produces a large upfield chemical shift while the other environment produces a smaller downfield shift. At room temperature these sites are in fast exchange but can be distinguished by either direct HgI_3^- competition or by the use of temperature to discriminate between the different binding kinetics at each site. We associate the upfield shifted resonance with the proximal binding cavity and have calculated the rate of exchange to be 2×10^7 M^{-1} s^{-1} with an approximate activation barrier of 16 kcal/mol.

(2) Methemoglobin in solution has only a single kinetically resolved binding environment. This environment produces a downfield shift similar to that observed for the second site in metmyoglobin. From previous X-ray crystallographic studies this site is localized in the A–B and G–H helix corner region. The estimated rate of exchange with this site is 6×10^7 M^{-1} s^{-1} with an approximate activation barrier of 13 kcal/mol.

Acknowledgments

We are pleased to acknowledge helpful conversations with Vladimir J. Basus, David Case, Fred Cohen, Hans Frauenfelder, and Benno Schoenborn. We thank Neil Bartlett for an initial gift of xenon. We also thank Vladimir J. Basus and Harold Melling for valuable technical assistance.

References

Antonini, E., & Brunori, M. (1971) *Hemoglobin and Myoglobin in Their Reactions with Ligands*, American Elsevier, New York.

Austin, R. H., Beeson, K. W., Eisenstein, L., Frauenfelder, H., & Gunsalus, I. C. (1975) *Biochemistry 14*, 5355–5373.

Bluhm, M. M., Bodo, G., Dintzis, H. M., & Kendrew, J. C. (1958) *Proc. R. Soc. London, Ser. A 246*, 369–389.

Breslow, E. (1964) *J. Biol. Chem. 239*, 486–496.
Conn, H. L., Jr. (1961) *J. Appl. Physiol. 16*, 1065–1070.
Emsley, J. W., Feeny, J., & Sutcliffe, L. H. (1965) *High Resolution Nuclear Magnetic Resonance Spectroscopy*, Vol. 1, Pergamon Press, Oxford.
Ewing, G. J., & Maestas, S. (1970) *J. Phys. Chem. 74*, 2341–2344.
Frauenfelder, H., Petsko, G. A., & Tsernoglou, D. (1979) *Nature (London) 280*, 558–563.
Kretsinger, R. H., Watson, H. C., & Kendrew, J. C. (1968) *J. Mol. Biol. 31*, 305–314.
Lakowicz, J. R., & Weber, G. (1973) *Biochemistry 12*, 4161–4179.
Miller, K. W., Reo, N. V., Uiterkamp, A., Stengle, D. P., Stengle, T. R., & Williamson, K. L. (1981) *Proc. Natl. Acad. Sci. U.S.A. 78*, 4946–4949.
Parkhurst, L. (1979) *Annu. Rev. Phys. Chem. 30*, 503–546.
Samejima, T., & Yang, J. T. (1964) *J. Mol. Biol. B*, 863–871.
Schoenborn, B. P. (1965) *Nature (London) 208*, 760–762.
Schoenborn, B. P. (1969) *J. Mol. Biol. 45*, 297–303.
Schoenborn, B. P., Watson, H. C., & Kendrew, J. C. (1965) *Nature (London) 207*, 28–30.
Schulman, R. G., Peisach, J., & Wyluda, B. J. (1970) *J. Mol. Biol. 48*, 517–523.
Smith, D. W., & Williams, R. J. P. (1968) *Biochem. J. 110*, 297–301.
Sudmeier, J. L., Evelhoch, J. L., & Jonsson, B. H. (1980) *J. Magn. Reson. 40*, 377–390.

Temperature-Dependent Molecular Motions of Cholesterol Esters: A Carbon-13 Nuclear Magnetic Resonance Study†

Geoffrey S. Ginsburg, Donald M. Small, and James A. Hamilton*

ABSTRACT: Carbon-13 NMR spectroscopy at 50.3 MHz has been used to study four long-chain cholesterol esters with a double bond in the ω-9 position: cholesteryl oleate, $C_{18:1}$, ω-9; cholesteryl linoleate, $C_{18:2}$, ω-6,9; cholesteryl erucate, $C_{22:1}$, ω-9; cholesteryl nervonate, $C_{24:1}$, ω-9. The linoleate and oleate esters exhibit two metastable liquid-crystalline phases (cholesteric and smectic), whereas the longer chain esters form a stable smectic phase but no cholesteric phase [Ginsburg, G. S., & Small, D. M. (1981) *Biochim. Biophys. Acta 664*, 98–107]. Line widths ($\nu_{1/2}$), spin–lattice relaxation times (T_1), and nuclear Overhauser enhancements (NOE) were measured for all well-resolved resonances from ring and fatty acyl (FA) carbons at different temperatures in the isotropic liquid of each ester. T_1 and NOE values of FA resonances were constant between the FA-2 carbon and olefinic region of each acyl chain and increased markedly for carbons near the chain terminus. FA carbon motions are thus restricted and/or highly correlated in the region between the ring and the olefinic carbons, suggesting that strong interactions occur between cholesterol ester molecules in this region of the FA chain. These results also suggest that the FA chains are approximately extended in the isotropic liquid. Steroid ring methine C-6 and C-3 $\nu_{1/2}$'s increased differentially on cooling to the liquid → liquid crystal transition temperature (T_m) of each ester, indicative of increasingly anisotropic ring rotations. The rotational anisotropy was quantitated by using a prolate ellipsoid model for the cholesterol ester molecule for which two correlation times (corresponding to rotations about the long and short molecular axes) were calculated from the C-3 and C-6 $\nu_{1/2}$ values. The C-3/C-6 $\nu_{1/2}$ ratio was directly proportional to the anisotropy of the ring motions as measured by the ratio of the two correlation times. At any given temperature relative to T_m, the C-3 and C-6 $\nu_{1/2}$'s and the C-3/C-6 $\nu_{1/2}$ ratios were larger for cholesterol esters which have a cholesteric phase than for esters which have no cholesteric phase, showing that steroid ring motions were more restricted and more anisotropic prior to the formation of a cholesteric phase. Cholesteryl erucate and cholesteryl nervonate have longer regions of FA chain interactions which result in greater chain cooperativity, apparently preventing the preordering of steroid rings to the degree necessary for formation of a cholesteric phase. Thus, these esters form the smectic phase directly from the isotropic liquid. These results are applied to the cholesterol ester transition in plasma low-density lipoproteins.

The physical state of cholesterol esters at physiological temperatures may be an important determinant in the development of atherosclerosis (Small, 1970). In systems such as cholesterol ester rich lipoproteins and atheromatous lesions, the cholesterol esters (primarily cholesteryl linoleate and cholesteryl oleate) undergo a phase transition from a smectic to a disordered phase at or above body temperature (Deckelbaum et al., 1975; Tall et al., 1978; Katz et al., 1976). However, in isolated pure systems, these cholesterol esters not only have slightly higher transition temperatures but also exhibit an additional intermediate cholesteric phase (Small, 1970; Ginsburg & Small, 1981). Elucidation of the factors which affect the phase behavior and transition temperature of pure cholesterol esters is thus important in order to understand the phase behavior of cholesterol esters in biological systems.

Several studies have shown that the domain size (Armitage et al., 1977) and the fatty acid composition of pure cholesterol esters influence their phase behavior (Small, 1970; Ginsburg & Small, 1981). In biological systems, such as plasma low-density lipoproteins (LDL),[1] the presence of other lipids such

† From the Biophysics Institute, Boston University Medical Center, 80 East Concord Street, Boston, Massachusetts 02118. *Received May 11, 1982.* This work was supported by U.S. Public Health Service Grants HL07291 and HL26335. A preliminary account of this work was presented at the 26th Annual Meeting of the Biophysical Society (Hamilton et al., 1982).

[1] Abbreviations: LDL, low-density lipoprotein; NMR, nuclear magnetic resonance; T_1, spin–lattice relaxation time; $\nu_{1/2}$, line width in hertz; NOE, nuclear Overhauser enhancement; Me_4Si (TMS in the figures), tetramethylsilane; FA, fatty acyl; C, cholesteryl ring carbons (standard steroid nomenclature used); T_m, temperature of the highest liquid → liquid crystal transition.

0006-2960/82/0421-6857$01.25/0